Research Square

Preprints are preliminary reports that have not undergone peer review.
They should not be considered conclusive, used to inform clinical practice,
or referenced by the media as validated information.

Safety and feasibility of Claudin18.2 (CLDN18.2)-specific CAR-NK cells in advanced gastrointestinal cancers: a phase 1 trial

Liu Yang

yangliu@hmc.edu.cn

Zhejiang provincial people's hospital

Yupeng Hong

Zhejiang Provincial People's Hospital

Zheling Chen

Zhejiang provincial people's hospital

Yang Gao

Zhejiang provincial people's hospital

Wen Lei

the SecondAffiliated Hospital, College of Medicine,Zhejiang University

Yaojie Pan

Zhejiang Provincial People's Hospital

Xiaochen Chen

Zhejiang Provincial People's Hospital

Peng Zhang

Zhejiang Provincial People's Hospital

Qian Ye

Hangzhou Rong-Gu Biotechnology Limited Company

Wenbin Qian

the Second Affiliated Hospital, College of Medicine, Zhejiang University https://orcid.org/0000-0002-9817-6674

Brief Communication

Keywords:

Posted Date: August 31st, 2026

DOI: https://doi.org/10.21203/rs.3.rs-10489398/v1

License: This work is licensed under a Creative Commons Attribution 4.0 International License.
Read Full License

Additional Declarations: There is **NO** Competing Interest.

Abstract

Despite advances in immunotherapy, outcomes for patients with advanced solid tumors remain unsatisfactory, and the clinical application of CAR-NK cells in this setting has not yet been reported. This phase 1, single-arm, open-label trial evaluated the safety and tolerability of CLDN18.2-BBz CAR-NK cells, an allogeneic CLDN18.2-targeted CAR-NK cell product incorporating 4-1BB and IL-15, in patients with refractory gastrointestinal cancers. After lymphodepleting chemotherapy, each patient received three intravenous infusions of the CAR-NK product at escalating-dose levels. Nine advanced patients (66.7% had received ≥ 2 prior lines) were consecutively enrolled and followed for a median of 14.9 months. The primary endpoint was safety and tolerability, and secondary endpoints included efficacy, pharmacokinetics and pharmacodynamics. No dose-limiting toxicities, cytokine release syndrome, immune effector cell-associated neurotoxicity, or graft-versus-host disease were observed, confirming a favorable safety profile. Disease control was achieved in 88.9% of patients, all of whom had stable disease, and notably one patient with pancreatic cancer maintained durable disease stabilization for 11 months. Pharmacokinetics revealed transient CAR-NK expansion in vivo. Single-cell profiling uncovered post-infusion peripheral immune remodeling: $CD8^+$ TEM cells established interactions with monocytes, recruiting them into the network while receiving inhibitory signals from myeloid cells, and reinforced crosstalk with proliferating $CD8^+$ T cells to support their expansion. These findings indicate that our allogeneic CAR-NK approach is well tolerated and provides meaningful disease stabilization, but the observed myeloid-derived inhibitory signals may contribute to resistance mechanisms, and future strategies should focus on enhancing CAR-NK persistence and counteracting immunosuppression to improve efficacy. ClinicalTrials.gov identifier: NCT06464965.

Introduction

The landscape of chimeric antigen receptor (CAR) T-cell therapy, once largely confined to hematological malignancies, is now expanding into solid tumors, fueled by recent landmark trials[1-3]. Nevertheless, multiple hurdles persist, including lengthy production timelines, immunosuppressive tumor microenvironments (TME), antigen heterogeneity or antigen loss, and T cell exhaustion[4-6]. These persistent limitations have driven extensive research into CAR-modified natural killer (CAR-NK) cells. Such constructs leverage the intrinsic anti-tumor potency of NK cells, while conferring key advantages including a lower incidence of cytokine release syndrome (CRS), freedom from major histocompatibility complex (MHC) restriction, and the capacity for off-the-shelf allogeneic cell therapy[7-11].

Between July 2024 and August 2025, we carried out a phase I clinical trial enrolling adult patients diagnosed with advanced gastric or pancreatic adenocarcinoma, who received infusions of CLDN18.2-targeted CAR-NK cells. The CAR-NK product was engineered to express a second-generation chimeric antigen receptor specific for tumor-cell-expressed claudin 18.2 (ClinicalTrials.gov identifier: NCT06464965). Notably, this second-generation CAR cassette integrates the 4-1BB co-stimulatory domain alongside interleukin-15 (IL-15), termed CLDN18.2-BBz CAR-NK. All participants underwent

lymphodepleting chemotherapy prior to cell infusion, comprising cyclophosphamide (500 mg m^{-2} per day, administered on days −5 to −3) and fludarabine (30 mg m^{-2} per day, administered on days −5 to −3). No bridging therapy or additional antitumor treatments were permitted before CAR-NK cell infusion. Nevertheless, salvage therapy was accessible for patients who experienced disease progression as determined by post-infusion efficacy evaluation. Patients received dose-escalated infusions of CLDN18.2-BBz CAR-NK cells on days 0, 3, and 7 at doses of 2×10^6, 8×10^6, and 1.6×10^7 CAR-positive NK cells per kilogram of body weight, respectively. The primary study endpoints were the maximum tolerated dose (MTD) and dose-limiting toxicity (DLT) of CLDN18.2-BBz CAR-NK cells. Secondary endpoints encompassed comprehensive evaluations of antitumor efficacy, including objective response rate (ORR), disease control rate (DCR), progression-free survival (PFS), overall survival (OS), and duration of response (DOR), as well as the in vivo expansion and persistence of CAR-NK cells in peripheral blood. Herein, we report the clinical safety profile, antitumor efficacy, CAR-NK cell kinetic characteristics, serum cytokine signatures, and single-cell RNA sequencing (scRNA-seq) results of peripheral blood immune cells from patients treated with CLDN18.2-specific CAR-NK cell therapy.

A total of nine patients with advanced digestive system malignancies were enrolled in this study. All eligible patients fulfilled the predefined inclusion criteria, including confirmation of CLDN18.2-positive tumor tissues via immunohistochemistry (IHC), an Eastern Cooperative Oncology Group (ECOG) performance status of 0 or 1, and a history of at least one prior line of standard systemic therapy. The CLDN18.2 IHC positivity was stratified by staining intensity and proportion[3]: low expression (intensity 1+ staining with any proportion or <40% tumor cells with any intensity), medium expression (40%–69% of tumor cells with intensity 2+ or 3+ staining), and high expression (≥70% of tumor cells with intensity 2+ or 3+ staining). Key exclusion criteria comprised prior treatment with CLDN18.2-targeted agents within 3 months before enrolment, active autoimmune disorders, uncontrolled systemic infections, central nervous system metastases, and active gastrointestinal ulceration or hemorrhage. Detailed exclusion criteria are fully listed in the Methods section. Among the nine enrolled subjects, three (33.3%) were diagnosed with gastric cancer (GC) and six (66.7%) with pancreatic adenocarcinoma (PC). All patients presented with metastatic disease, and two-thirds (6/9, 66.7%) had received ≥2 lines of prior systemic anti-tumor therapy. The median patient age was 66 years (range, 38–73). The cohort was predominantly female (7 out of 9, 77.8%), and the vast majority of participants exhibited an ECOG performance status of 1 (8/9, 88.9%). Comprehensive baseline demographic and clinical characteristics are summarized in Extended Data Table 1,2.

No pre-specified dose-limiting toxicities (DLTs) were documented within the 28-day observation window following the initial CAR-NK infusion, and the maximum tolerated dose (MTD) was not attained. As summarized in Extended Data Table 3, the most prevalent grade ≥3 adverse events (AEs) were myelosuppressive toxicities secondary to lymphodepleting conditioning regimens, observed across all nine patients (100%). These hematological toxicities comprised grade ≥3 leucopenia in seven participants (77.8%), neutropenia in six (66.7%), anemia in four (44.4%), and thrombocytopenia in two (22.2%). Notably, no cases of CRS, immune effector cell-associated neurotoxicity syndrome (ICANS), or other cell therapy-related neurotoxicity were recorded. With respect to on-target off-tumor

gastrointestinal toxicity, no grade ≥3 gastrointestinal AEs emerged. A single patient developed grade1 gastrointestinal hemorrhage, which fully resolved following standard supportive care. Other frequently encountered AEs included hyponatremia (7/9, 77.8%; one grade 3 episode), reduced appetite (8/9, 88.9%; all grade 1–2), pyrexia (7/9, 77.8%; all grade 1–2), elevated aspartate aminotransferase (AST; 7/9, 77.8%; all grade 1–2), and raised alanine aminotransferase (ALT; 5/9, 55.6%; all grade 1–2).

Tumor assessments were conducted at baseline, on day 28 following the final CAR-NK infusion, and every eight weeks thereafter until disease progression, in accordance with the RECIST (Response Evaluation Criteria in Solid Tumors) version 1.1 criteria. No objective tumor responses were achieved across the nine enrolled patients. The best overall response comprised stable disease (SD) in eight patients (88.9%) and progressive disease (PD) in one patient (11.1%), corresponding to a DCR of 88.9%. At the data cutoff date of June 30, 2026, the median progression-free survival (PFS) and overall survival (OS) of the entire cohort were 2.0 months and 11.0 months, respectively (Fig. 1a–c). Subgroup analysis stratified by tumor type revealed distinct clinical outcomes. Among three patients with gastric cancer (GC), two achieved SD and one developed PD, yielding a DCR of 66.7% and a median PFS of 1.5 months. By contrast, all six patients with pancreatic cancer (PC) attained SD, resulting in a 100% DCR and a median PFS of 2.0 months. Of particular note, one PC patient (Patient 3, treated at the lowest dose level of 2×10^6 cells per kg) maintained sustained SD for 11 months, representing the longest disease control duration in this cohort. This patient harbored low CLDN18.2 expression (1+ staining, 50% tumor cells), presented with bone and lymph node metastases, and carried wild-type KRAS. They received only one prior line of first-line tegafur–gimeracil–oteracil therapy, which was discontinued due to treatment intolerance. An additional PC patient (Patient 6, dosed at 8×10^6 cells per kg) with high CLDN18.2 expression (3+ staining, 90% tumor cells) and KRAS mutation achieved a PFS of 5 months.

Following infusion, CAR^+ NK cells underwent in vivo expansion, with a median peak expansion time of 3 days (range, 3–8 days). The peak frequency of circulating CAR^+ NK cells ranged from 0.24% to 38.31% (median, 4.90%), with two patients (Patient 5 and Patient 6) achieving robust CAR-NK expansion exceeding 30% (Fig.1d). Nevertheless, CAR-NK persistence was relatively limited. Circulating CAR^+ cells became undetectable (defined as <0.1%) in most patients by day 14 post-infusion. Notably, one patient (Patient 6) retained detectable CAR^+ cells (0.84%) at day 25, while another (Patient 7) maintained measurable levels (0.73%) at day 16 (Fig.1e). No significant correlations were observed between the administered cell dose (2×10^6 to 1.6×10^7 cells per kg) and peak CAR-NK expansion or persistence. Similarly, no clear associations existed between peripheral CAR-NK kinetic profiles and clinical therapeutic outcomes. Digital droplet PCR (ddPCR) confirmed the presence of CAR transgene copies in patients who achieved disease control. Specifically, Patient 3 with durable SD exhibited low-level but long-term CAR transgene persistence, with detectable CAR copies remaining positive at day 270. In addition, Patient 6 with sustained SD harbored high levels of CAR DNA copies at day 149.

Longitudinal serum cytokine profiling revealed predominantly mild and transient cytokine elevations following CAR-NK infusion. Key cytokines implicated in CRS, including IL-6 and IFN-γ, exhibited only moderate, patient-dependent increases relative to baseline (peak IL-6: 0.09–11.79-fold change; peak

IFN-γ: up to 15.1-fold change). IL-10 displayed sporadic elevation spikes, such as a 55.8-fold increase observed in Patient6 on day 7, yet these increases were unsustained. By contrast, IL-5 and TNF-α levels remained largely stable near baseline across most patients (Extended Data Fig.1a). Consistent with the absence of high-grade CRS, systemic inflammatory markers, including C-reactive protein, D-dimer, and ferritin, presented only mild fluctuations throughout the treatment course (Extended Data Fig. 1b). No significant correlations were identified between cytokine elevation magnitudes and treatment-related adverse events, including the low-grade pyrexia observed in 70% of patients. This blunted cytokine response profile highlights the favorable safety characteristics of CLDN18.2-specific CAR-NK therapy, distinctly differentiating it from the severe cytokine-driven toxicities commonly associated with conventional CAR-T cell therapy[12,13]. Although no objective tumor regression was achieved in this cohort, the attainment of durable disease stabilization—including a remarkable 11-month sustained SD in one pancreatic cancer patient—represents a clinically meaningful outcome. Collectively, these preliminary results demonstrate tangible biological activity of allogeneic CLDN18.2 CAR-NK cells in heavily pretreated patients with advanced digestive malignancies, as reflected by an overall DCR of 88.9%. Meanwhile, the lack of objective partial or complete responses underscores the necessity for further optimization of CAR-NK product design, dosing regimens, or combinatorial therapeutic strategies to enhance antitumor potency.

To explore how CLDN18.2-CAR-NK cell infusion reshapes the peripheral immune microenvironment, we performed single-cell RNA sequencing (scRNA-seq) on paired pre- and post-infusion peripheral blood mononuclear cell (PBMC) samples from three representative patients (Patients 7, 8, and 9). A total of 83,062 high-quality cells were included in the final transcriptional profiling. Unsupervised clustering delineated all major immune cell lineages, encompassing T cells, NK cells, monocytes/macrophages, neutrophils, dendritic cells (DCs), and B cells (Fig.2a). CAR-NK infusion triggered profound remodeling of the peripheral immune landscape (Fig. 2b–d). The relative proportion of circulating T/NK cells declined markedly from 88.0% to 48.0%, while the monocyte/macrophage compartment underwent dramatic expansion, rising from 4.3% to 44.9%. Notable compositional and functional remodeling was also observed across T cell subsets (Fig. 2e,f). Effector memory $CD8^+$ T cells (CD8_TEM) expanded from 25.2% to 35.3%, and proliferative $CD8^+$ T cells (ProCD8_T) increased 7.6-fold from 1.9% to 14.5%. The expansion of effector T cell populations was coupled with a pronounced reduction in naive T cell compartments: the frequency of naive $CD4^+$ T cells (CD4_Tn) dropped from 31.0% to 15.8%, and naive $CD8^+$ T cells (CD8_Tn) were almost undetectable post-infusion (from 2.2% to 0.4%). In comparison, the overall proportion of NK cells remained largely stable, decreasing slightly from 16.4% to 14.2%. To quantitatively evaluate T cell functional status, we calculated canonical gene signature scores using predefined gene sets. Post-infusion $CD8^+$ T cells displayed significantly elevated signature scores for both activation and cytotoxicity (marked by IFNG, GZMB, PRF1, and NKG7), as well as T cell exhaustion (characterized by PDCD1, HAVCR2, TIGIT, and LAG3)[14,15] (Extended Data Fig.2a, b). By contrast, NK cells exhibited substantially enhanced activation and cytotoxicity signatures (encompassing NKG7, GNLY, PRF1, GZMB, and FCGR3A) after infusion, while gene signatures associated with NK cell suppression

and functional impairment (TIGIT, HAVCR2, CBLB, SOCS1, and TGFBR1) remained statistically unchanged[16,17].

We next characterized transcriptional heterogeneity within the monocyte/macrophage compartment. Subclustering analysis identified three canonical monocyte subsets, including classical monocytes (cMo), intermediate monocytes (iMo), and non-classical monocytes (ncMo) (Fig. 2g). Notably, post-infusion immune profiles were significantly enriched for monocyte subsets harboring high expression of MHC class II molecules and interferon-stimulated genes. Conversely, monocyte subpopulations defined by high ZEB2 and LYZ expression were markedly diminished after CAR-NK treatment (Fig. 2h).

To delineate the alterations in cell-cell interactions among immune cells, we conducted CellChat analysis to compare outgoing and incoming signaling patterns across distinct immune cell populations (Extended Data Fig. 2c-j). At baseline, CD8_TEM cells predominantly participated in lymphocyte–lymphocyte crosstalk, communicating with CD4_Tn cells and NK cells. Following CAR-NK cell treatment, this communication landscape underwent substantial remodeling. CD8_TEM cells established robust interactions with monocytes, recruiting these cells into the immune communication network, while monocytes simultaneously delivered inhibitory signaling inputs to CD8_TEM cells. In parallel, CD8_TEM cells reinforced their crosstalk with proliferating CD8+T cells, thereby supporting the expansion of this T cell subset.

These results suggest that the concurrent presence of myeloid-derived inhibitory signals and T cell proliferative signals may underpin the activation and exhaustion signatures characteristic of T cells post treatment. Moreover, intercellular communication networks mediated by MHC molecules exhibited prominent rewiring upon CAR-NK cell infusion. Specifically, MHC-I signaling was markedly enhanced between CD8_TEM cells and proliferating ProCD8 T cells, as well as between CD8_TEM cells and cMo-NAMPThi monocytes. Similarly, strengthened MHC-II signaling was observed in the interactions between CD8_TEM cells and ProCD8 T cells, and between CD8_TEM cells and monocyte subpopulations (Extended Data Fig. 2g–j).

The recently completed phase 2 trial of satra-cel (CT041), a CLDN18.2-targeted CAR-T therapy, has demonstrated significant PFS benefits over physician's choice chemotherapy in heavily pretreated patients with CLDN18.2-positive advanced gastric or gastroesophageal junction cancers[1]. These findings firmly validate CLDN18.2 as a clinically viable target for cellular immunotherapy against gastrointestinal malignancies. Nevertheless, several bottlenecks continue to hinder the widespread clinical implementation of CLDN18.2 CAR-T therapy, including intricate manufacturing procedures and a 95% incidence rate of CRS[18]. Here, we report the phase 1 clinical outcomes of CLDN18.2-specific CAR-NK cell therapy. Our results reveal a favorable safety profile and promising disease control efficacy in heavily pretreated patients with advanced gastric and pancreatic cancers, with a DCR of 88.9% and a median OS of 11.0 months. Collectively, CLDN18.2 CAR-NK cells represent a promising off-the-shelf cellular therapeutic alternative with a unique safety landscape, which may overcome the key limitations of current CAR-T treatment.

In our phase I study, CLDN18.2-targeted CAR-NK cells yielded modest antitumor activity, with no objective responses recorded despite a DCR of 88.9%. This efficacy profile contrasts sharply with that observed in the satra-cel CAR-T trial, which reported a confirmed ORR of 22% and a median PFS of 9.07 months in the CAR-T treatment group[1]. Multiple key factors may underlie this inter-trial efficacy discrepancy. First, differences in patient selection based on CLDN18.2 expression levels may have compromised therapeutic efficacy. Only 55.6% of patients in our cohort exhibited high CLDN18.2 expression, compared with 77% of participants in the satra-cel trial[1]. Given that high CLDN18.2 expression is correlated with improved survival outcomes in the CT041-ST-01 trial, the lower proportion of high-expression patients in our study likely diminished the probability of achieving objective responses and durable PFS. Second, the limited in vivo persistence of CAR-NK cells constitutes a critical efficacy-limiting factor. Unlike CAR-T cells, which exert sustained long-term cytotoxic activity, the CAR-NK cells in our study peaked at an early time point (median of 3 days) and became undetectable in the majority of patients by day 14. Of note, two patients achieved durable SD: Patient3 maintained SD for 11 months and Patient 6 attained a 5-month PFS. Their prolonged disease stabilization was associated with low-level CAR-DNA persistence at day 270 and day 149 post-treatment respectively, indicating that rare long-term CAR-NK residency may facilitate tumor stabilization.

Four landmark clinical trials, including the CD19-BBz (4-1BB) CAR-NK study[19], cord blood-derived CAR19/IL-15 CAR-NK trial[20], cryopreserved TAK-007 trial[21], and iPSC-derived FT596 trial[22], have collectively validated the safety and clinical efficacy of allogeneic CAR-NK therapy in B-cell lymphoma. These studies consistently demonstrated a favorable safety profile characterized by minimal CRS, absent ICANS and GvHD, with ORRs ranging from 49% to 63%. Nevertheless, complete remission (CR) rates (27–50%) and long-term disease control achieved by CAR-NK therapy remain inferior to those of benchmark autologous CD19 CAR-T therapies. Recent single-cell studies have further elucidated the cellular and molecular mechanisms underlying CAR-NK therapeutic resistance[19,23]. Li et al. demonstrated that CAR-NK cells undergo progressive metabolic dysfunction following tumor recognition, with gradual attenuation of glycolysis and oxidative phosphorylation activity. This metabolic impairment drives the emergence of dysfunctional CAR-NK subpopulations characterized by hypoxic and inflammatory signatures, enabling metabolically hyperactive tumor clones to outcompete immune cells and ultimately trigger tumor relapse[23]. In parallel, the CD19-BBz (4-1BB) CAR-NK trial revealed that treatment responders predominantly harbor a less differentiated, proliferative CAR-NK subset with robust immune effector potential. In contrast, non-responders exhibit enriched matured and exhausted CAR-NK clusters, accompanied by elevated CBLB-mediated ubiquitination and TGF-β-driven immunosuppression within the TME[19]. Collectively, these findings indicate that CAR-NK resistance is not merely attributed to the short in vivo half-life of CAR-NK cells but arises from a combination of intrinsic immune metabolic exhaustion, unfavorable cellular subset distribution, and tumor microenvironment-mediated immune suppression. Consistent with these mechanistic insights, our scRNA-seq results revealed that CLDN18.2-targeted CAR-NK infusion expands endogenous CD8 T cells while concurrently inducing T cell exhaustion signatures. Moreover, monocyte populations were significantly expanded and established inhibitory crosstalk with T cells post-treatment. This immune dysregulation pattern

recapitulates the TGF-β-mediated immunosuppression and T cell dysfunction reported in previous CAR-NK resistance studies[19]. Taken together, our results suggest that CAR-NK therapy-induced immune activation is counteracted by myeloid-derived immune suppression and subsequent T cell exhaustion, highlighting the tumor TME as a pivotal barrier to sustained CAR-NK therapeutic efficacy[7].

In conclusion, to the best of our knowledge, this study represents the first-in-human clinical investigation of CLDN18.2-targeted CAR-NK cell therapy for advanced gastrointestinal malignancies. The treatment exhibited an excellent safety profile with zero incidences of CRS, ICANS, or GvHD, and achieved durable disease control in the majority of enrolled patients. While no objective tumor responses were observed, the prolonged stable disease attained in individual patients indicates that CLDN18.2 CAR-NK cells can confer tangible clinical benefits in a subset of patients with advanced gastrointestinal cancers. These findings strongly warrant further optimization of CAR-NK cell persistence and cytotoxic potency. Additionally, our results support future combinatorial therapeutic strategies that target and reverse TME-mediated immunosuppression, thereby overcoming the resistance mechanisms identified in this study and improving the long-term efficacy of CAR-NK immunotherapy.

Declarations

Acknowledgements

We appreciate all patients and their families for supporting this study. Sponsors have no role in study design, data collection and analysis or paper writing. This work was supported by funds from the Clinical Multi-center Research Project of Zhejiang Provincial People's Hospital (2025DZX001), National Natural Science Foundation of China (82373308), Leading Goose Project of Science and Technology Department of Zhejiang Province (2024 C03089), Key research and development program of Zhejiang Province(2025C01105).

Author contributions

Liu Yang and Wenbin Qian designed the study. Wenbin Qian’s team produced the CAR-NK cells. Yupeng Hong, Zheling Chen, Yang Gao, Yaojie Pan, Xiaochen Chen,Peng Zhang enrolled, treated patients, and collected the data. Yupeng Hong, Zheling Chen, Yang Gao,Wenbin Qian and Liu Yang analyzed and interpreted data. Yupeng Hong, Wenbin Qian and Liu Yang drafted the paper. All authors read and approved the final paper, provided feedback throughout the development process, and approved the final submitted version.

Competing interests

All authors declare no competing interests.

Data availability

The raw sequence data reported in this paper have been deposited in the Genome Sequence Archive in National Genomics Data Center, China National Center for Bioinformation / Beijing Institute of Genomics, Chinese Academy of Sciences (GSA-Human: HRA020013) that are publicly accessible at https://ngdc.cncb.ac.cn/gsa-human/browse/HRA020013.In compliance with the Chinese Human Genetic Resources Administration Regulations, the raw sequencing data are available under controlled access in accordance with Genome Sequence Archive (GSA) controlled management regulations. Access to the data can be requested by completing the application form via GSA-Human System and is granted by the corresponding Data Access Committee. Additional guidance can be found at the GSA-Human System website (https://ngdc.cncb.ac.cn/gsa-human/document/GSA-Human_Request_Guide_for_Users_us.pdf). The clinical trial study protocol is available in the Supplementary Information file. Source data are provided with this paper. Individual patient-level clinical data cannot be made publicly available because the informed consent obtained from participants did not include provisions for public data sharing, and the release of such detailed data could compromise participant privacy even after de-identification. However, de-identified individual participant clinical data may be made available to qualified researchers upon reasonable request to the corresponding author, subject to institutional review and the execution of a data-sharing agreement. No custom code was used in this study. All bioinformatics and statistical analyses were performed using standardized commercial or open-source software as detailed in the Methods section.

References

1. Qi, C., *et al.* Claudin-18 isoform 2-specific CAR T-cell therapy (satri-cel) versus treatment of physician's choice for previously treated advanced gastric or gastro-oesophageal junction cancer (CT041-ST-01): a randomised, open-label, phase 2 trial. *Lancet (London, England)* 405, 2049–2060 (2025).
2. Qi, C., *et al.* CT041 CAR T cell therapy for Claudin18.2-positive metastatic pancreatic cancer. *Journal of hematology & oncology* 16, 102 (2023).
3. Qi, C., *et al.* Claudin18.2-specific CAR T cells in gastrointestinal cancers: phase 1 trial interim results. *Nature medicine* 28, 1189–1198 (2022).
4. Du, B., *et al.* CAR-T therapy in solid tumors. *Cancer cell* 43, 665–679 (2025).
5. Brudno, J.N., Maus, M.V. & Hinrichs, C.S. CAR T Cells and T-Cell Therapies for Cancer: A Translational Science Review. *Jama* 332, 1924–1935 (2024).
6. Lamplugh, Z.L., Wellhausen, N., June, C.H. & Fan, Y. Microenvironmental regulation of solid tumour resistance to CAR T cell therapy. *Nature reviews. Immunology* 26, 230–248 (2026).
7. Biederstädt, A. & Rezvani, K. Engineered natural killer cells for cancer therapy. *Cancer cell* 43, 1987–2013 (2025).
8. Biederstädt, A., *et al.* Genome-wide CRISPR screens identify critical targets to enhance CAR-NK cell antitumor potency. *Cancer cell* 43, 2069–2088.e2011 (2025).

9. Zhang, B., *et al.* Chimeric antigen receptor-based natural killer cell immunotherapy in cancer: from bench to bedside. *Cell Death Dis* 15, 50 (2024).
10. Gong, Y., Klein Wolterink, R.G.J., Wang, J., Bos, G.M.J. & Germeraad, W.T.V. Chimeric antigen receptor natural killer (CAR-NK) cell design and engineering for cancer therapy. *Journal of hematology & oncology* 14, 73 (2021).
11. Jørgensen, L.V., Christensen, E.B., Barnkob, M.B. & Barington, T. The clinical landscape of CAR NK cells. *Exp Hematol Oncol* 14, 46 (2025).
12. Brudno, J.N. & Kochenderfer, J.N. Current understanding and management of CAR T cell-associated toxicities. *Nature reviews. Clinical oncology* 21, 501–521 (2024).
13. Mulvey, A., Trueb, L., Coukos, G. & Arber, C. Novel strategies to manage CAR-T cell toxicity. *Nature reviews. Drug discovery* 24, 379–397 (2025).
14. Zheng, L., *et al.* Pan-cancer single-cell landscape of tumor-infiltrating T cells. *Science* 374, abe6474 (2021).
15. Azizi, E., *et al.* Single-Cell Map of Diverse Immune Phenotypes in the Breast Tumor Microenvironment. *Cell* 174, 1293–1308.e1236 (2018).
16. Tang, F., *et al.* A pan-cancer single-cell panorama of human natural killer cells. *Cell* 186, 4235–4251.e4220 (2023).
17. Crinier, A., *et al.* High-Dimensional Single-Cell Analysis Identifies Organ-Specific Signatures and Conserved NK Cell Subsets in Humans and Mice. *Immunity* 49, 971–986.e975 (2018).
18. Qi, C., *et al.* Claudin18.2-specific CAR T cells in gastrointestinal cancers: phase 1 trial final results. *Nature medicine* 30, 2224–2234 (2024).
19. Lei, W., *et al.* Safety and feasibility of 4-1BB co-stimulated CD19-specific CAR-NK cell therapy in refractory/relapsed large B cell lymphoma: a phase 1 trial. *Nature cancer* 6, 786–800 (2025).
20. Marin, D., *et al.* Safety, efficacy and determinants of response of allogeneic CD19-specific CAR-NK cells in CD19(+) B cell tumors: a phase 1/2 trial. *Nature medicine* 30, 772–784 (2024).
21. Darrah, J.M., *et al.* A Phase 2, Open-Label, Multicenter Study of the Safety and Efficacy of TAK-007 in Adult Patients with Relapsed/Refractory B-cell Non-Hodgkin Lymphoma. *Blood Cancer Discov* (2026).
22. Ghobadi, A., *et al.* Induced pluripotent stem-cell-derived CD19-directed chimeric antigen receptor natural killer cells in B-cell lymphoma: a phase 1, first-in-human trial. *Lancet (London, England)* 405, 127–136 (2025).
23. Li, L., *et al.* Loss of metabolic fitness drives tumor resistance after CAR-NK cell therapy and can be overcome by cytokine engineering. *Sci Adv* 9, eadd6997 (2023).

Methods

1. Single-cell sequencing

1.1 Single cell isolation from blood

For blood samples requiring PBMC isolation, extraction was performed according to the manufacturer's instructions for Histopaque®-1077 (10771, Sigma-Aldrich) and Ficoll (F4375, Sigma-Aldrich). Liquid samples were transferred to 15mL centrifuge tubes. Cells were resuspended in 400μL of PBS containing 0.1% BSA, followed by the addition of 4 mL of 1× Red Blood Cell Lysis Solution (MACS 130-094-183, Miltenyi Biotec). The mixture was gently inverted for homogenization and placed on ice for 10 minutes. The reaction was terminated by adding 4 mL of PBS with 0.1% BSA for dilution, and the sample was centrifuged at 100g for 7 minutes at 12 °C. After centrifugation, the supernatant was discarded, and the cell pellet was resuspended in 1 mL of PBS (with 0.1% BSA) by gentle pipetting. Then, 5mL of PBS (with 0.1% BSA) was added, and the mixture was inverted 5–6 times for thorough mixing. The sample was centrifuged again at 100g for 7 minutes at 12 °C. The resuspension and centrifugation steps were repeated twice. Finally, the cell pellet was resuspended at an appropriate volume of PBS (with 0.1% BSA) according to the pellet size and kept on ice. Cells were stained with Acridine Orange–Propidium Iodide (AO-PI), mixed thoroughly by pipetting, and counted using a CountStar automated cell counter.

1.2 Library Construction and Sequencing for 10X Single-Cell 3' Transcriptomics

Ten thousand cells were loaded into the Chromium Controller (10X Genomics, PN-120270) on a Chromium Single Cell B Chip (10X Genomics, PN-1000690) and processed to generate single-cell gel beads in the emulsion (GEM) according to the manufacturer’s protocol (10X Genomics, CG000183). cDNA amplification and library construction were performed using Chromium Single Cell 3’ Reagent Kits v4 (10XGenomics, PN1000691) according to the manufacturer's manual. Quality control for constructed library was conducted by Agilent dsDNA 915 Reagent kit(35-5000bp) (Agilent, DNF-915-K0500) for qualitative analysis. Quantification analysis was performed by VAHTS Library Quantification Kit for Illumina (VAHTS, NQ101). The resulting libraries were sequenced on the Illumina NovaSeq 6000 sequencing system with 2×150 paired-end kits using the following read length: 28 bp Read1 for cell barcode and UMI, 8 bp I7 index for sample index, and 91 bp Read2 for transcript a minimum depth of 20,000 reads per cell.

1.3 Data Preprocessing and Quality Control

Raw sequencing data were converted to FASTQ format using Illumina bcl2fastq (v5.0.1). Cell counting and gene expression profiling were performed with CellRanger (v9.0.1), and scRNA-seq data were aligned to the Ensembl GRCm39 reference genome. The processing pipeline was carried out with the support of LC-Bio.

1.4 Data Filtering and Cell Identification

Putative doublets were identified using Doublet Finder (v2.0.4). Subsequent downstream analysis was conducted with the Seurat package (v4.4.0). Low-quality cells detecting fewer than 500 genes or exhibiting >25% mitochondrial transcript content were excluded. After removing low-quality cells and

doublets, gene expression data were normalized using the NormalizeData function. Highly variable genes were identified via FindVariableFeatures, and data scaling was performed using ScaleData. Principal component analysis (PCA) was carried out with RunPCA, followed by cell clustering using FindNeighbors and FindClusters. Dimensionality reduction was performed using t-SNE (RunTSNE) and UMAP (RunUMAP), and clustering results were visualized with DimPlot.

During dimensionality reduction and clustering, batch effects were corrected using the RunHarmony function from the Harmony package (v1.1.0). Marker genes for each cluster were identified using FindAllMarkers with the following thresholds: $\log_2$FC > 0.26, p-value < 0.05 (bimod likelihood-ratio test), and expression in at least 10% of cells within the cluster. Enrichment analysis for the marker genes of each cluster was performed using OmicStudioClassic (v1.13.0). Cell types were annotated based on known marker genes and visualized using DotPlot and FeaturePlot.

2. **Manufacture of Claudin18.2 CAR-NK cells**

Human CB units for this study were provided by Zhejiang Blood Center Cord Blood Bank, which was approved by the Ethic Committee of Zhejiang Blood Center. All donors provided written informed consent. CAR-NK cell manufacture was performed in the GMP Laboratory of the Second Affiliated Hospital, College of Medicine, Zhejiang University.

$CD3^-$ CB mononuclear cells (CBMCs) were obtained from fresh cord blood using a RosetteSep-based CD3 depletion strategy according to the manufacture. Briefly, whole cord blood was transferred into tissue culture flasks and RosetteSep™ Human CD3 Depletion Cocktail (STEMCELL Technologies) was added at 50μL/mL of blood, followed by gentle mixing and incubation for 20 min at room temperature. The blood was then diluted 1:1 with normal saline and carefully layered onto Ficoll solution. After density-gradient centrifugation at 1,200×g for 20 min (low acceleration and no brake), the mononuclear cell layer was collected, washed twice, and residual erythrocytes were removed by red blood cell lysis. The resulting $CD3^-$ depleted CBMCs were counted and assessed by flow cytometry as $CD45^+CD3^-CD56^+$ subtypes.$CD3^-$CBMC were then frozen in liquid nitrogen as seed cells before further application.

When produce the CAR-NK cells, the $CD3^-$ CBMCs (< 0.1%) were stimulated with K562 feeder cells at a 2:1 ratio on day 0. Cells were maintained ImmunoCult-X-T cell Exp Medium (STEMCELL Technologies) with 5% CTS Immune Cell Serum Replacament (SR) and 100 IU/mL human IL-2 (Quangang). On day 6 of culture, phenotype of culture cells and feeder cells were detected by flow cytometry using Pacific Blue anti-human CD45 antibody (Biolegend, 304029, HI30), FITC anti-human CD56 antibody (Biolegend, 362546, 5.1H11), APC-Cy7 anti-human CD3 antibody (Biolegend, 300426, UCHT1), PE-Cy7 anti-human CD137L antibody (Biolegend, 311512, 5F4) and the detecting strategies are described in Supplementary Figure 1a. NK cells were subsequently transduced with a BaEV-LV encoding Claudin18.2 CAR with NGFR expression as a detecting marker at a multiplicity of infection of 8. Two days later, a second round of feeder cells stimulation was performed for CAR-NK cell expansion. On day 16, CAR-NK cells were harvested for clinical infusion. The phenotype of CAR-NK products were detected by APC anti-human

CD271 (NGFR) Antibody (345108 , ME20.4), FITC anti-human CD56 antibody (Biolegend, 362546, 5.1H11), PerCP anti-human CD16 antibody (Biolegend, 302030, 3G8), PE anti-human NKp46 (331908, 9E2), and PE-Cy7 anti-human NKp44 (325116, P44-8). The Release criteria were displayed in **Supplementary Table1** and **Supplementary Figure 1a.**

3. Detection of CAR-NK cells in peripheral blood by flow cytometry

To evaluate the proliferation and persistence of CAR-NK cells, CAR-positive NK cells in peripheral blood were analyzed using multiparameter flow cytometry. Briefly, whole blood samples were treated with FACS Lysing Solution (BD Biosciences) to lyse red blood cells. The remaining cells were washed and resuspended in phosphate-buffered saline (PBS) containing 2% fetal bovine serum (FBS) and 0.1% sodium azide (NaN_3). Cells were then stained for 15 minutes at room temperature with a panel of fluorescently labeled antibodies, including Pacific Blue-anti-CD45, APC/Cy7-anti-human CD3, APC anti-human CD271 (NGFR) Antibody (for CAR detection), FITC-anti-CD56. After staining, cells were washed by centrifugation at 400× g and data were acquired on a NovoCyte flow cytometer (ACEA Biosciences). Data analysis was performed using NovoExpress software (ACEA Biosciences). The panel of fluorescent antibodies used is presented in **Supplementary Table2** and the gating strategy is depicted in **Supplementary** Figure 1b.

4. **Monitoring of CAR-NK cells in blood by Digital-droplet PCR**

Digital-droplet PCR (ddPCR) was used to monitor the CAR-NK cell persistence in blood as previously described[1]. Due to the high concentration of internal reference genes, the two genes were separated into two independent reaction systems for better target gene (Claudin18.2) detection. The reaction mix was composed of 12.5μL of 2×ddPCR Universal Mastermix for DNA (with UDG, Maccura), 1.25μL FAM-labeled Claudin18.2 CAR primer-probe-assay, 0.1μL XbaI, 0.1μL Mlu I, 0.1μL HindIII-HF restriction enzyme (NEB), 10-660ng gDNA (volume 2~5μL), and nuclease-free water to a final volume of 25μL. The reaction was incubated for 15 min at 37 °C for restriction digestion, and then droplets were generated. The ddPCR was run using a D 600 Digital PCR System(Maccura) with the cycling conditions as follows: initial denaturation at 95 °C for 5 min, amplification with 45 cycles at 95 °C for 20 s, and 60 °C for 30 s. The ramp rate was set to 2.0 °C /s. Finally, droplets were analyzed, and data was processed with Digital PCR System, including Poisson's distribution analysis that enables absolute quantification of the target. The copies of target gene per droplet were calculated based on the number of negative droplets in the sample. Data of absolute copies/μL of the target gene in the sample volume was calculated with the formula: Z (copies/μL) =X × 25 (total volume) /Y (sample volume). X: the quantitative value provided by the D 600 Digital PCR system; Y: the input sample volume; Z: the sample concentration. The concentration of each internal reference gene was calculated by multiplying the output result with the dilution ratio 125. Then, the copies/μL of the internal reference gene were converted to μg/μL through the following formula: A (μg/μL) =B (copies/μL) × 3.3/1000000. Finally, the quantitative values of target gene were calibrated with the corresponding quantitative values of the internal reference genes as Z

(Claudin18.2 CAR, copies/μL) / A (internal reference gene, μg/μL). Primers for Claudin 18.2 CAR are following:

Forword: 5’-ACAGGTCCCCGGAAAAGAA-3’;

Reverse:5’- TGTCCTGGCTGATGGTGAAT-3’;

Probe: GGCATCTCCGCCTCTAGCGGCCGCA

Promers for human actin are:

Forword: 5’- TCCGTGTGGATCGGCGGCTCCA-3’

Reverse: 5’-CTGCTTGCTGATCCACATCTG-3’

Probe: CCTGGCCTCGCTGTCCACCTTCCA

Phase I clinical trial

5.1 Study Design and Participants

This phase I, single-center, single-arm, open-label trial was designed to evaluate the safety and preliminary efficacy of Claudin18.2-targeted, umbilical cord blood-derived CAR-NK cells (CB CAR-NK18.2) in patients with advanced gastric or pancreatic adenocarcinoma who had failed or were intolerant to standard therapies. The study protocol received approval from the Ethics Committee of Zhejiang Provincial People’s Hospital and was registered at ClinicalTrials.gov (identifier: NCT06464965; registration date: June 13, 2024). In compliance with the Declaration of Helsinki, all participants provided written informed consent for both trial participation and publication of clinical data. Commercial insurance covering potential study-related injuries was provided to each participant by Asia-Pacific Property & Casualty Insurance Co., Ltd. Patient enrollment commenced on July 3, 2024, and concluded on August 31, 2025. Sex-based analyses were not conducted. The complete study protocol is available in the Supplementary Information.

Prior to cell infusion, patients underwent lymphodepleting chemotherapy with cyclophosphamide (500 mg/m²/day from day −5 to day −3) and fludarabine (30 mg/m²/day from day −5 to day −3). Bridging therapies or additional anti-tumor treatments following infusion were prohibited. Escalating doses of CB CAR-NK18.2 cells were administered via intravenous infusions on days 0, 3, and 7, at dose levels of 2×10^6, 8×10^6, and 1.6×10^7 CAR-positive NK cells per kilogram of body weight, respectively.

Key eligibility criteria comprised: age 18–75 years; histologically confirmed advanced gastric or pancreatic adenocarcinoma with progression on or intolerance to standard treatment; an Eastern Cooperative Oncology Group performance status of ≤1; an absolute neutrophil count ≥2,000/μL; a platelet count ≥50,000/μL; and adequate renal, hepatic, and cardiac function. A major exclusion criterion was prior treatment with any Claudin18.2-directed cellular therapy (e.g., CAR-T, CAR-NK, TCR-T) within

three months before study enrollment. Detailed inclusion and exclusion criteria are provided in Supplementary Clinical Study Protocol.

5.2 Endpoints

The co-primary endpoints were to determine the maximum tolerated dose (MTD) and dose-limiting toxicities (DLTs) of CB CAR-NK18.2. Cytokine release syndrome (CRS) was graded according to the American Society for Transplantation and Cellular Therapy consensus criteria, while other adverse events were assessed using the Common Terminology Criteria for Adverse Events (CTCAE, version 5.0). Secondary efficacy endpoints included objective response rate (ORR), disease control rate (DCR), progression-free survival (PFS), overall survival (OS), and duration of response (DOR). Exploratory objectives involved assessing the expansion and persistence of CAR-NK cells in peripheral blood. Tumor response was evaluated radiologically based on the Response Evaluation Criteria in Solid Tumors (RECIST), version 1.1. Patients with primary or metastatic brain tumors were excluded at baseline. The first post-treatment tumor assessment was scheduled for approximately day 28 after the initial cell infusion.

5.3 Statistical Analysis

Given the exploratory nature of this Phase I trial focused on safety and initial response evaluation, study variables were summarized primarily using descriptive statistics. Dose escalation followed a standard 3 + 3 design to establish the MTD. Time-to-event endpoints, including PFS and OS, were estimated using the Kaplan-Meier method. PFS was defined as the time from the first CB CAR-NK18.2 infusion to disease progression or death from any cause; OS was defined as the time from the first infusion to death from any cause. No data were excluded from the analyses. The study was not randomized, and investigators were not blinded to treatment allocation or outcome assessment.

Reference

1. Mika, T., et al. Digital-Droplet PCR for Quantification of CD19-Directed CAR T-Cells. Front Mol Biosci 7, 84 (2020).

Figures

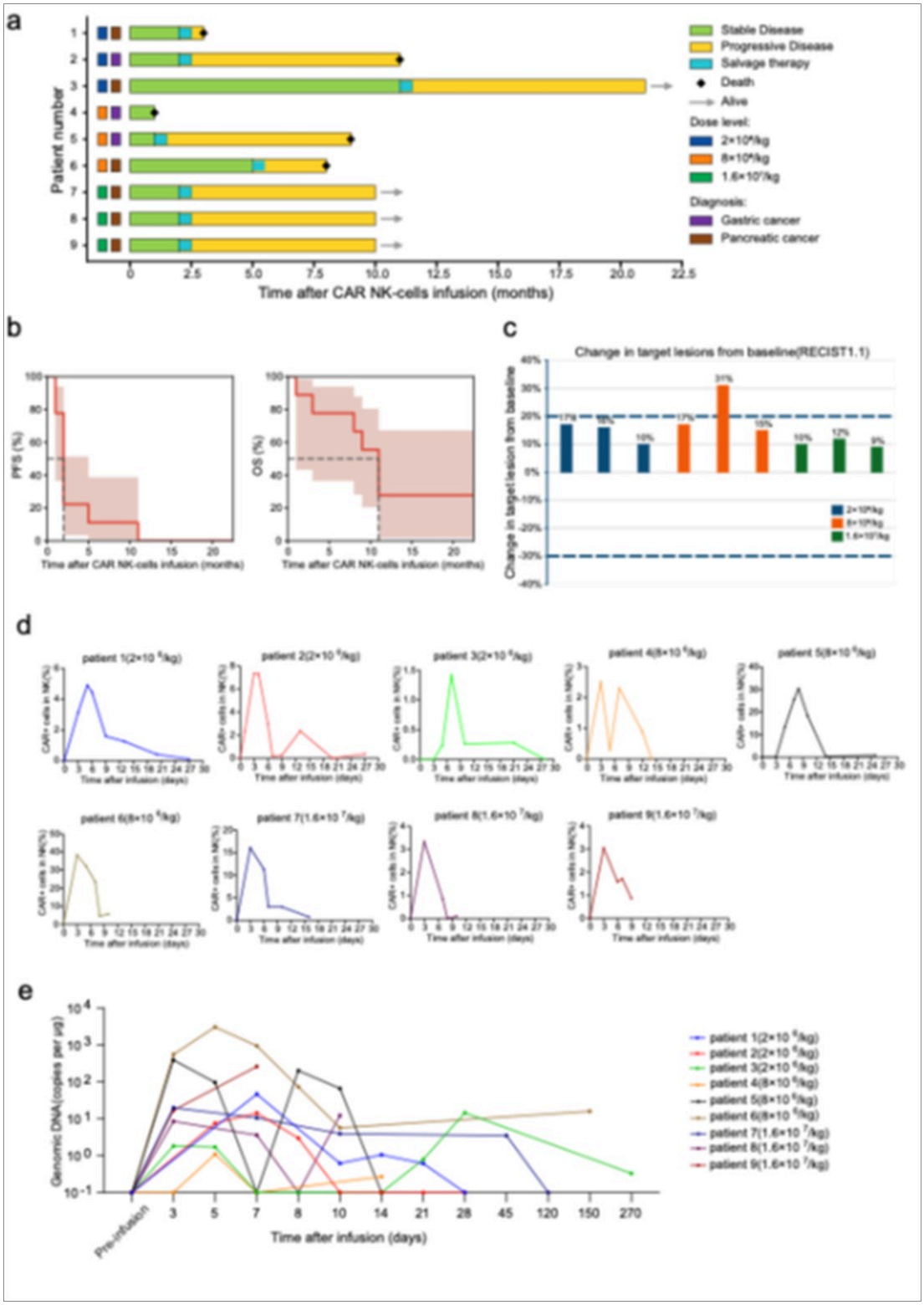


Figure 1

Antitumor activity and CAR-NK cell kinetics. (a) Swimmer plot illustrating longitudinal clinical outcomes for all enrolled patients (n = 9). Each horizontal bar spans the period from CAR-NK cell infusion to the final disease evaluation, with colored segments indicating dynamic disease status (stable disease or progressive disease). Color-coded boxes at the start of each bar denote the administered dose level (2 × 10^6/kg, 8 × 10^6/kg or 1.6 × 10^7/kg) and tumor type (gastric cancer or pancreatic cancer). Black

diamonds represent patient death events, and gray arrows indicate patients alive at the last follow-up. (b) Kaplan–Meier survival analysis for progression-free survival (PFS) and overall survival (OS) across the entire cohort (n = 9), with a median PFS of 2.0 months and a median OS of 11.0 months. Solid red curves depict the Kaplan–Meier survival estimates, shaded areas represent 95% confidence intervals, and dashed horizontal lines mark the median survival endpoints. (c) Waterfall plot displaying the best percentage change from baseline in the summed diameters of target lesions per RECIST v1.1 criteria for individual patients. Bars are stratified by dose cohort, with horizontal dashed lines indicating the RECIST-defined thresholds for progressive disease (+20%) and partial response (−30%). (d) Circulating CAR-positive NK cell kinetics following infusion (n = 9). CAR-positive NK cells in peripheral blood were quantified via flow cytometry, with longitudinal changes in the proportion of CAR-positive cells within the NK cell compartment plotted against days post-infusion. (e) Kinetics of genetically modified CAR-NK cells in peripheral blood measured by ddPCR. Each individual panel corresponds to a single patient, with the administered dose level annotated accordingly. Abbreviations: PFS, progression-free survival; OS, overall survival; RECIST, Response Evaluation Criteria in Solid Tumors.

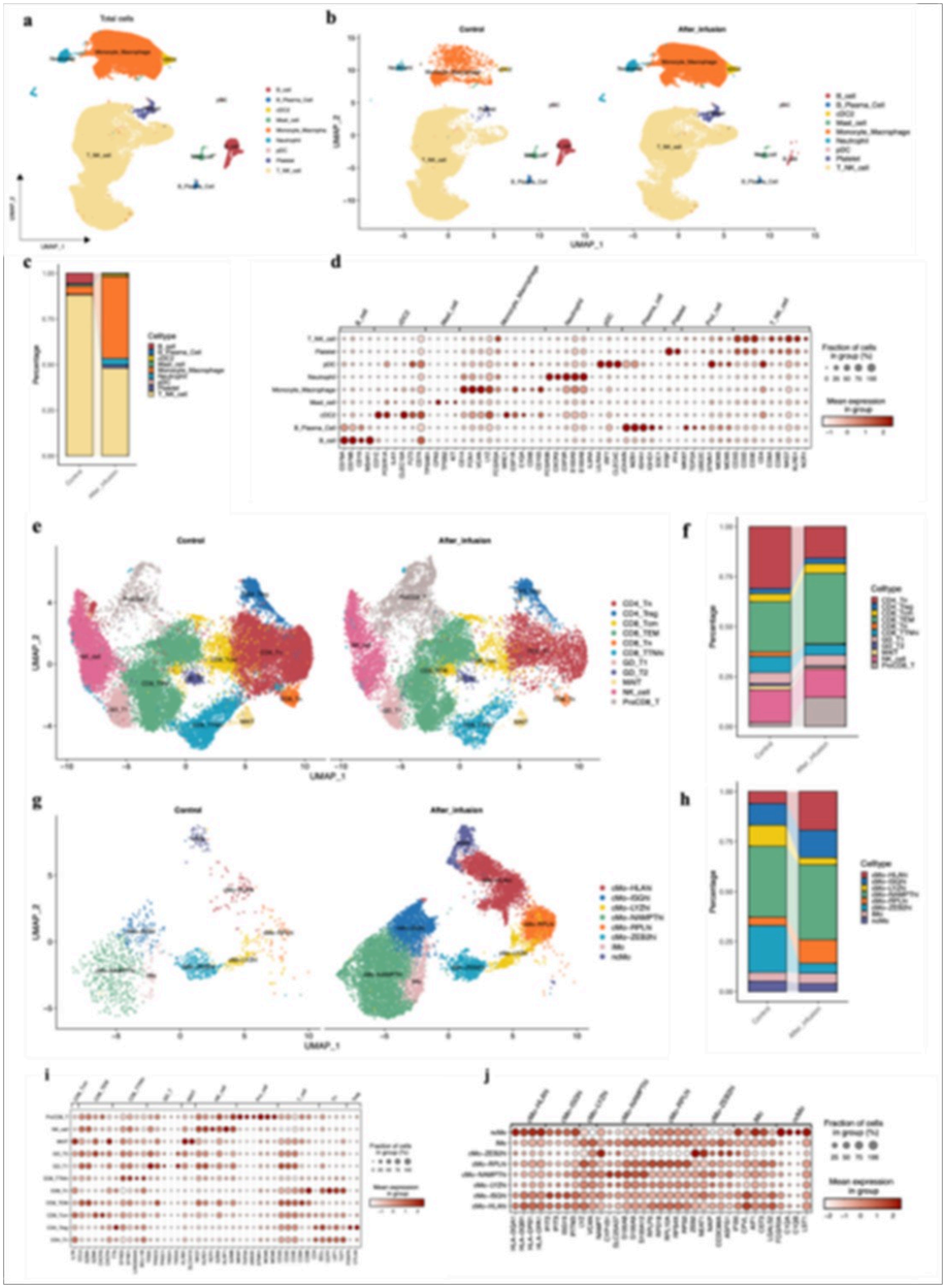


Figure 2

Single-cell transcriptional profiling of peripheral immune cells from CAR-NK-treated patients. (a) UMAP visualization of transcriptomic profiles for 83,062 cells derived from paired peripheral blood mononuclear cell (PBMC) samples collected pre- and post-CLDN18.2-CAR-NK infusion from three representative patients (P7, P8, P9). Unsupervised clustering delineated nine major immune cell lineages. (b) UMAP embedding of peripheral immune cells from paired PBMC samples at baseline (Day

0, control) and post-infusion (Day 7) across the three representative patients (P7, P8, P9). (c) Stacked bar graphs illustrating dynamic proportions of major immune cell subsets before and after CAR-NK cell infusion. (d) Dot plot displaying the expression levels of canonical marker genes across the annotated immune cell populations. (e) UMAP visualization of subclustered T and NK cell populations derived from paired pre- and post-infusion PBMC samples. (f) Stacked bar plots showing proportional changes in T/NK cell subsets following CAR-NK infusion. (g) UMAP visualization of subclustered monocyte and macrophage populations from paired pre- and post-infusion PBMC samples. (h) Stacked bar graphs depicting the dynamic proportions of monocyte and macrophage subsets before and after CAR-NK treatment. (i,j) Dot plots presenting the expression levels of signature marker genes for the indicated immune cell subsets.

Supplementary Files

This is a list of supplementary files associated with this preprint. Click to download.

- SupplementaryfileClinicalStudyProtocol.docx
- Supplementarymaterial.docx
- ExtendedData.docx